JAMES | Journal of Advances in Modeling Earth Systems

RESEARCH ARTICLE
10.1029/2021MS002590

A Universal Approach for the Non-Iterative Parametrization of Near-Surface Turbulent Fluxes in Climate and Weather Prediction Models

V. M. Gryanik[1,2], C. Lüpkes[1], D. Sidorenko[1], and A. Grachev[3]

[1]Alfred-Wegener-Institut Helmholtz-Zentrum für Polar- und Meeresforschung, Bremerhaven, Germany, [2]A. M. Obukhov Institute of Atmospheric Physics, Russian Academy of Sciences, Moscow, Russia, [3]Boundary Layer Research Team, Atmospheric Dynamics & Analytics Branch, DEVCOM Army Research Laboratory, WSMR, Las Cruces, NM, USA

Key Points:

- A non-iterative universal parameterization of surface layer turbulent fluxes is derived using Monin-Obukhov similarity theory
- Bulk transfer coefficients are given, which are based on five pairs of state-of-the-art surface layer stability functions
- The new parametrizations provide a basis for a cheap study of the impact of surface layer turbulent fluxes in numerical weather prediction and climate models

Correspondence to:
C. Lüpkes,
christof.luepkes@awi.de

Citation:
Gryanik, V. M., Lüpkes, C., Sidorenko, D., & Grachev, A. (2021). A universal approach for the non-iterative parametrization of near-surface turbulent fluxes in climate and weather prediction models. *Journal of Advances in Modeling Earth Systems*, *13*, e2021MS002590. https://doi.org/10.1029/2021MS002590

Received 22 APR 2021
Accepted 12 JUL 2021

Abstract Weather prediction and climate simulations need reliable parameterizations of turbulent fluxes in the stable surface layer. Especially in these conditions, the uncertainties of such parametrizations are still large. Most of them rely on the Monin-Obukhov similarity theory (MOST), for which universal stability functions (SFs) represent important ingredients. The SFs are nonlinear, if so, a numerical iteration of the MOST equations is required. Moreover, presently available SFs are significantly different at large stability. To simplify the calculations, a non-iterative parametrization of fluxes is derived and corresponding bulk transfer coefficients for momentum and heat for a package of five pairs of state-of-the-art SFs are proposed. For the first time, a parametrization of the related transfer coefficients is derived in a universal framework for all package members. The new parametrizations provide a basis for a cheap systematic study of the impact of surface layer turbulent fluxes in weather prediction and climate models.

Plain Language Summary Results of weather forecast, present-day climate simulations, and future climate projections depend among other factors on the interaction between the atmosphere and the underlying sea-ice, the land, and the ocean. In numerical weather prediction and climate models, some of these interactions are accounted for by transport coefficients describing the turbulent exchange of momentum, heat, and humidity. Currently used transfer coefficients have, however, large uncertainties in flow regimes being typical for cold nights and seasons, but especially in the polar regions. Furthermore, their determination is numerically complex. It is obvious that progress could be achieved when the transfer coefficients would be given by simple mathematical formula in frames of an economic computational scheme. Such a new universal, so-called non-iterative parametrization scheme is derived for a package of transfer coefficients. The derivation is based on the Monin-Obukhov similarity theory, which is well accepted in the scientific community. The new scheme provides a basis for a cheap systematic study of the impact of near-surface turbulence and of the related transports of momentum, heat, and humidity in models.

1. Introduction

Parametrizations of surface layer turbulent fluxes used in numerical weather prediction (NWP) and climate models describe the impact of the unresolved turbulent mixing of momentum, heat, and humidity on resolved physical processes. Especially important is the parametrization of the turbulent fluxes in the stable surface layer (SSL) in polar regions, see for example, Louis et al. (1982) (LTG82), Gryanik and Lüpkes (2018) (GL18), and Gryanik et al. (2020) (GLGS20), and references therein. In numerical atmospheric models as, for example, in the WRF model (Jiménez et al., 2012), the regional climate model HIRHAM5 (Christensen et al., 2007) and in coupled atmosphere-ocean models like ECHAM6-FESOM (Sidorenko et al., 2015), the turbulent transports of momentum, heat, and humidity in the surface layer are usually described by Monin-Obukhov similarity theory (MOST, Monin & Obukhov, 1954). It connects the surface boundary conditions with the lowest model level above the surface. One of the important ingredients of MOST are universal stability functions (SFs, often called ϕ_m and ϕ_h-functions). These functions, correspondingly the stability correction functions (SCFs, ψ_m and ψ_h-functions, sometimes also called integral SFs) are nonlinear,

so that the solution of the MOST equations for the calculation of fluxes requires circumstantial iteration. It is obvious that non-iterative parametrizations of fluxes are preferable.

The method for deriving such non-iterative parametrizations can be traced back to Deardorff (1968). It provides bulk transfer coefficients as functions of the bulk Richardson number Ri_b (defined by Equation 10 below) and of the roughness parameters for momentum $\epsilon_m = z/z_0$ and heat $\epsilon_t = z/z_t$, where z is the distance to the underlying surface, z_0 is the surface aerodynamic roughness length scale and z_t is the length scale for heat. Recently, GL18 and GLGS20 improved the method and derived new non-iterative parametrizations of fluxes using the SFs of Grachev et al. (2007) (in the following GAFGP07) and of GLGS20 as a basis. However, there are many other SFs, which are used in contemporary numerical models. Here our main goal is to consider a package of those SFs, which are the most often used ones in climate and weather prediction models. These are the SFs suggested by Businger et al. (1971), Dyer (1974) (in the following BD), Holtslag and De Bruin (1988), Beljaars and Holtslag (1991), and Cheng and Brutsaert (2005) (in the following HB88, BH91 CB05, respectively) and by GLGS20. For the definitions of all these SFs, we refer to the original papers, but in Section 3) we present the corresponding SCFs, which are in our main interest. For the physical and mathematical properties of these SFs and SCFs, we refer to the original papers and also to those of, for example, Andreas (2002), Sharan and Kumar (2011), Srivastava and Sharan (2019), GLGS20, and references therein. Thus, to our first and main goal, we derive new non-iterative parametrizations of bulk transfer coefficients based on the different sets of SFs.

Different kinds of applications of the new parameterizations in models are possible. In combination with an iterative scheme, the non-iterative parametrization can significantly reduce the numerical costs, when it is used to determine the first guess values (e.g., Grachev & Fairall, 1997). The package might be used in single-function mode when an existing iterative scheme shall be replaced by a more efficient non-iterative one. But the most promising is to apply the different transfer coefficient schemes in an aggregated way (Bou-Zeid et al., 2020, and references therein). Namely, in the same model, some of the package members can be applied to regions covered by sea ice (GL18 and GLGS20) and simultaneously, other ones to land surfaces (LTG82, HB88, BH91, and CB05) and to the ocean (LTG82, HB88, GL18, and GLGS20). Recently Schneider (2020) performed simulations with HIRHAM5, a state-of-the-art regional atmospheric model, using only two members of the package: the non-iterative parametrization of GL18 over sea ice, but the default ones of LTG82 everywhere else. However, until today climate models are using different default parametrizations, for example, those based on HB88, BH91, and CB05 SFs. For this reason, the second goal of this work is the introduction of non-iterative surface flux parametrizations as a package, where for the first time, the parametrizations of transfer coefficients are represented all by formula of the same universal functional form, which is well suited for practical use in NWP and climate models.

In addition, keeping in mind that modeling of the Arctic is one of the bottlenecks in current state-of-the-art Earth system modeling (Jung et al., 2016), we present exemplarily the impact of the atmospheric SSL on the turbulent fluxes of momentum and heat for Arctic conditions. To that aim, we considered three issues. First, using Era Interim data as a basis, we estimated the typical frequency of occurrence of SSLs, by selecting one month and several days being typical for Arctic early spring. Second, we estimated the typical difference in transfer coefficients for different members of the package by selecting one representative day with large frequency of occurrence of very SSLs (large Ri_b). Finally, we considered the geographic distribution of these differences between transfer coefficients. This example may motivate further systematic studies of the impact of different SSLs (represented by different SFs) in NWP and climate models by using then the new, less cpu-time consuming non-iterative parametrizations (separately or combined with iterative schemes, see Section 2).

2. Bulk Parametrization Based on MOST

Bulk formulations of the turbulent tangential surface stress $\vec{\tau}$ (stress magnitude τ, often called vertical flux of momentum) and of the sensible heat flux H read as

$$\vec{\tau} = -\rho C_d |\vec{U}(z)| \vec{U}(z), \quad H = -\rho\, c_p C_h |\vec{U}(z)| [\Theta_v(z) - \Theta_0]. \tag{1}$$

Here, $\vec{U}(z) = (U(z),0)$ is the mean wind speed, which is taken to be zero at the underlying surface, Θ_v is the mean virtual potential temperature, Θ_0 is its surface value. Using the virtual potential temperature assumes that the turbulent mixing is the same for humidity as for temperature (Reynolds analogy for scalars), thus $C_q = C_t$, where C_q and C_t are the transfer coefficients for humidity and for temperature, respectively. C_d and C_h are the transfer coefficients for momentum (drag coefficient) and heat, c_p is specific heat at constant pressure. Height z is located in the surface layer but above the roughness sublayer ($\epsilon_m \gg 1, \epsilon_t \gg 1$).

Assuming that the turbulence is statistically quasi-stationary and fluxes are independent on height above an underlying horizontally homogeneous surface, MOST provides the mean wind speed profiles $U(z)$ and mean virtual potential temperature profiles $\Theta_v(z)$ as

$$U(z) = \frac{u_*}{\kappa}\left[\ln\epsilon_m - \psi_m\left(\zeta\right) + \psi_m\left(\zeta/\epsilon_m\right)\right], \tag{2}$$

$$\Theta_v(z) - \Theta_0 = \frac{\theta_*}{\kappa}\left[Pr_0 \ln\epsilon_t - \psi_h\left(\zeta\right) + \psi_h\left(\zeta/\epsilon_t\right)\right] \tag{3}$$

with the von Kàrmàn constant $\kappa = 0.4$ and the neutral-limit turbulent Prandtl number Pr_0. Here, $\psi_m(\zeta)$ and $\psi_h(\zeta)$ are MOST SCFs for momentum and heat, $\zeta = z/L$ is the MOST stability parameter with the Obukhov length $L = u_*^2/\kappa(g/\theta_v)\theta_*$, where $u_*^2 = \tau/\rho$ and $\theta_* = -H/(\rho c_p)u_*$ are the characteristic friction velocity and characteristic temperature scale, g is the acceleration due to gravity. The SCFs $\psi_m(\zeta)$ and $\psi_h(\zeta)$ define the diabatic corrections to the mean wind speed and mean virtual potential temperature. The neutral contributions are represented by logarithmic terms depending on the roughness parameters ϵ_m and ϵ_t. The SCFs are negative for stable stratification ($\psi_m < 0, \psi_h < 0$), positive for unstable conditions ($\psi_m > 0, \psi_h > 0$), and $\psi_m(0) = \psi_h(0) = 0$ for the neutral case.

The transfer coefficients C_d and C_h in Equation 1 are given as

$$C_d = C_{dn} f_m, \quad C_h = C_{hn} f_h, \tag{4}$$

$$C_{dn} = \frac{\kappa^2}{\ln^2\epsilon_m}, \quad C_{hn} = \frac{\kappa^2}{Pr_0 \ln\epsilon_m \ln\epsilon_t}, \tag{5}$$

where C_{dn} and C_{hn} are the transfer coefficients for neutral stratification, and f_m and f_h are the corresponding normalized transfer coefficients for momentum and heat, respectively. According to an approach of GL18, the f_m and f_h are provided by the semi-analytical solution of the MOST Equations 1–3 as

$$f_m = \left[1 - \frac{\psi_m(\zeta)}{\ln\epsilon_m}\right]^{-2}, \tag{6}$$

$$f_h = \left[1 - \frac{\psi_m(\zeta)}{\ln\epsilon_m}\right]^{-1}\left[1 - \frac{\psi_h(\zeta)}{Pr_0 \ln\epsilon_t}\right]^{-1} \tag{7}$$

with

$$\zeta(Ri_b,\epsilon_m,\epsilon_t) = C\,Ri_b + A\,Ri_b^{\gamma}, \tag{8}$$

$$C = \frac{\ln^2\epsilon_m}{\ln\epsilon_t}, \quad A = \frac{(\ln\epsilon_m - \psi_{ma})^{2(\gamma-1)}}{\zeta_a^{\gamma-1}(\ln\epsilon_t - \psi_{ha})^{\gamma-1}}\left[\frac{(\ln\epsilon_m - \psi_{ma})^2}{\ln\epsilon_t - \psi_{ha}} - \frac{\ln^2\epsilon_m}{\ln\epsilon_t}\right], \tag{9}$$

$\psi_{ma} = \psi_m(\zeta_a), \psi_{ha} = \psi_h(\zeta_a)$, and

$$Ri_b = \frac{g}{\theta_v}\frac{(\Theta_v(z)-\Theta_0)z}{|\vec{U}(z)|^2}, \quad Ri_b \geq 0, \tag{10}$$

the bulk Richardson number. Here, γ and ζ_a are constants, which can be determined numerically by a least-square fit to the exact solution of the MOST equations using the metric of relative error for $\zeta(Ri_b, \ln\epsilon_m, \ln\epsilon_t)$. The semi-analytical solution approaches the exact solution at $\zeta \to 0$ if $\gamma > 1$, and it coincides with the exact solution at $\zeta = \zeta_a$ assuming that $1/\epsilon_k \ll 1$, and $\psi_k(\zeta_a/\epsilon_k) \ll \psi_k(\zeta_a)$, where $k = [m,h]$.

Equations 4–10 define a general non-iterative parametrization of the fluxes (1) in terms of the bulk Richardson number Ri_b and roughness parameters ϵ_m and ϵ_t for any reasonable SF when SCFs are specified and the constants γ and ζ_a are derived. The parametrizations fulfill the following criteria, which are common for all high quality parametrizations:

1. They represent an accurate approximate solution of the set of MOST equations. The accuracy of approximation is compatible to the accuracy of measurement data.
2. The method used for their derivation is universally applicable to a package of SFs, not just to only one specific function.
3. The solutions should be obtained in the widest ranges of Ri_b, ϵ_m, and ϵ_t, which are available from measurements.
4. Transfer coefficients are continuous functions of Ri_b and both roughness parameters ϵ_m and ϵ_t.
5. They have the correct behavior in the limit of near-neutral and weak stability ($Ri_b \to 0$, practically $Ri_b < 0.1$), which is compatible with fluxes derived from Businger-Dyer SFs.
6. The parametrizations have a simple analytical functional form, which is well suited for the practical use in weather prediction and climate models.

3. A Package of SCFs

While there is a large selection of publications on SFs, we follow here the choice already motivated in Section 1, and give a summary of SCFs, which we included in our package for a detailed study. These are five pairs of SFs, namely those of BD, HB88, BH91, CB05, and GLGS20. For all but BD and GLGS20, the neutral-limit turbulent Prandtl number $Pr_0 = 1$.

1. BD SCFs read as

$$\psi_m(\zeta) = -a_m\zeta, \quad \psi_h(\zeta) = -Pr_0 a_h\zeta, \quad 0 \leq \zeta < 1, \tag{11}$$

   where a_m and a_h are empirical constants. The most representative values of empirical constants are $a_m = 5, a_h = 5$ and $Pr_0 = 1$.
2. HB88 SCFs are given as

$$\psi_m(\zeta) = \psi_h(\zeta) = -a\zeta - b\left(\zeta - \frac{c}{d}\right)\exp(-d\zeta) - \frac{bc}{d}, \quad 0 \leq \zeta < 10 \tag{12}$$

   with the four empirical constants $a = 0.7, b = 0.75, c = 5, d = 0.35$.
3. BH91 suggested the same SCF Equation 12 as HB88 for momentum, but propose a new function for heat, which is given as

$$\psi_h(\zeta) = -\left(1 + \frac{2a}{3}\zeta\right)^{3/2} + 1 - b\left(\zeta - \frac{c}{d}\right)\exp(-d\zeta) - \frac{bc}{d}, \quad 0 \leq \zeta < 10 \tag{13}$$

   with the same four constants $a = 1, b = 0.667, c = 5$ and $d = 0.35$ for both $\psi_m(\zeta)$ and $\psi_h(\zeta)$.
4. CB05 established SCFs as

$$\psi_k(\zeta) = -a_k \ln\left[\zeta + (1 + \zeta^{b_k})^{1/b_k}\right], \quad k = [m,h], \quad 0 \leq \zeta < 5. \tag{14}$$

   Values of the four empirical constants are: $a_m = 6.1, b_m = 2.5$ for momentum and $a_h = 5.3, b_h = 1.1$ for heat.

Table 1
The Package of Universal Non-Iterative Parametrizations for Stable Surface Layer Transfer Coefficients

	ζ_{max}	$Ri_{b,max}$	γ	ζ_a	Equations
BD	1	0.17	4.42	2.5	4–9, 11
HB88	10	0.37	2.14	4.0	4–9, 12
BH91	10	0.47	2.04	3.4	4–9, 12, 13
CB05	5	0.20	2.28	4.5	4–9, 14
GLGS20	100	0.41	3.62	7.25	4–9, 15, 16

Note. BD refers to the stability correction functions of Businger et al. (1971) and Dyer (1974). HB88, BH91, CB05, and GLGS20 refer to Holtslag and De Bruin (1988), Beljaars and Holtslag (1991), Cheng and Brutsaert (2005), and Gryanik et al. (2020), respectively. Columns are: (a) the maximal values of the MOST stability parameter ζ_{max}; (b) the corresponding $Ri_{b,max}$, for which the stability functions were originally established; (c) the constants γ and (iv) ζ_a, which are used in Equations 8 and 9; (d) the equations defining the corresponding parametrization for the transfer coefficients.

5. GLGS20 derived SCFs based on the functions of GAFGP07 but they represent extended and improved versions given by equations

$$\psi_m(\zeta) = -3\frac{a_m}{b_m}\left[(1 + b_m\,\zeta)^{1/3} - 1\right], \quad 0 \le \zeta < 100, \tag{15}$$

$$\psi_h(\zeta) = -Pr_0\frac{a_h}{b_h}\ln(1 + b_h\zeta), \quad 0 \le \zeta < 100 \tag{16}$$

with the neutral-limit Prandtl number $Pr_0 = 0.98$ and with four constants $a_m = 5.0$, $a_h = 5.0$, $b_m = 0.3$, and $b_h = 0.4$. These functions were constructed in order to fit the SHEBA (Surface Heat Energy Budget of the Arctic Ocean) data as close as possible. We remind the reader that SHEBA provides an excellent data set collected at five mast levels over about 1 year for polar conditions with frequent SSLs (GAFGP07 and references therein). For this reason, we will use the GLGS20 SCFs as reference functions in the following.

Note that all Equations 12–16 approach the BD functions at $\zeta \to 0$, but the empirical constants a_m and a_h are different for different functions. The strict applicability of the SFs of BD, HB88, and CB05 are limited to the range of small ζ (correspondingly, small Ri_b), see Table 1. However, in numerical models the parametrizations of transfer coefficients based on these SFs are often used for all values of ζ, far beyond the range, for which they were originally established.

4. New Parametrizations

After specifying $\psi_m(\zeta)$ and $\psi_h(\zeta)$ by Equations 11–16, we can easily find the optimal constants γ and ζ_a, using the least-square fitting method, as described in the previous section. The calculated values of these constants are given in Table 1 for all SFs. The ranges of Ri_b, ϵ_m and ϵ_t used for optimization are the same for all SCFs, namely the wide range $0 \le Ri_b < 0.4$ for stability, and for the roughness parameters $1.5\times10^3 \le \epsilon_m \le 3\times10^5$ and $\epsilon_m \le \epsilon_t \le 10^2\epsilon_m$. Based on $z = 10$ m this corresponds in terms of z_0 also to a variability over several magnitudes (3.3×10^{-5} m $\le z_0 \le 6.7\times10^{-3}$ m, $0.01z_0 \le z_t \le z_0$). These ranges as well as the given range of Ri_b are most common for polar sea ice regions, as documented by SHEBA and other campaigns (GAFGP07, GL18, and references therein).

Finally, plugging the constants γ and ζ_a in Equations 8 and 9, we obtain the new universal non-iterative parametrization of turbulent fluxes, which is expressed by Equations 1 and 4–10.

For all five members of the package the non-iterative parametrizations reproduce the exact f_m and f_h reasonably well. The level of accuracy is visible in Figure 1 showing results of the new parametrizations and of the iterative schemes for f_m and f_h as a function of Ri_b and using the average sea ice roughness parameters $\epsilon_m = 3\times10^4$ and $\epsilon_t = \epsilon_m$ / 0.7 (based on $z = 10$ m, $z_0 = 3.3\times10^{-4}$ m, $z_t = 0.7z_0$, see GL18 and GLGS20), but also for an extremely smooth (water) surface ($\epsilon_m = 10^7$, $z_0 = 10^{-6}$ m) and for a rough land surface ($\epsilon_m = 30$,

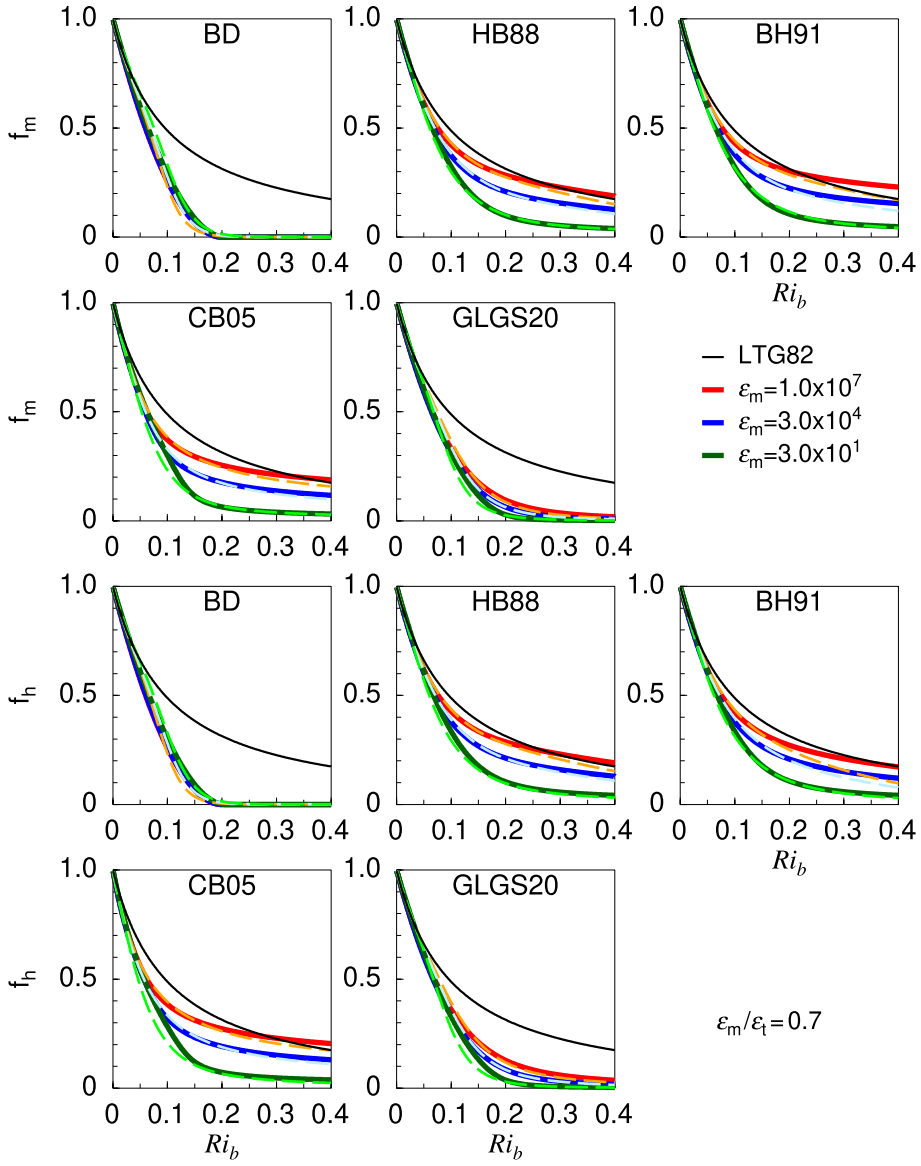

Figure 1. Normalized transfer coefficients f_m and f_h for momentum and heat as a function of Ri_b and dependent on the surface roughness parameters ϵ_m and ϵ_t with values as explained in the figure. Dashed lines refer to the iterative solutions, solid lines represent the non-iterative solutions. Blue lines represent typical sea ice conditions, the red solid and orange dashed lines are results for extremely smooth surfaces and the greenish curves represent rough land surfaces, see text. Black lines are the parametrization of LTG82.

$z_0 = 0.33$ m). The value 10^{-6} m (equivalent to a neutral drag coefficient at 10 m height of 0.6×10^{-4}) is not a typical value for the open ocean but can appear sometimes in calm conditions, for example, close to sea ice as measured by Elvidge et al. (2016) (see their Figure 3 and values for zero ice cover).

The maximum error is of about 10% ($Ri_b \leq 0.25$) and of about 15% (except BH91) for $0.25 < Ri_b < 0.4$. For BH91 the error is increasing between $Ri_b = 0.25$ and $Ri_b = 0.37$ for f_h to 30%. For $Ri_B > 0.2$ the values of f_m and f_h following from BD are zero by definition. We stress, that the iteratively obtained f_m and f_h functions are reproduced well in a much larger roughness range than that for sea ice.

The figure includes also the classical parametrization of LTG82:

$$f_m = \frac{1}{(1 + c_1\, Ri_b \,/\, \sqrt{1 + Ri_b})}, \qquad f_h = \frac{1}{(1 + c_2\, Ri_b \sqrt{1 + Ri_b})} \tag{17}$$

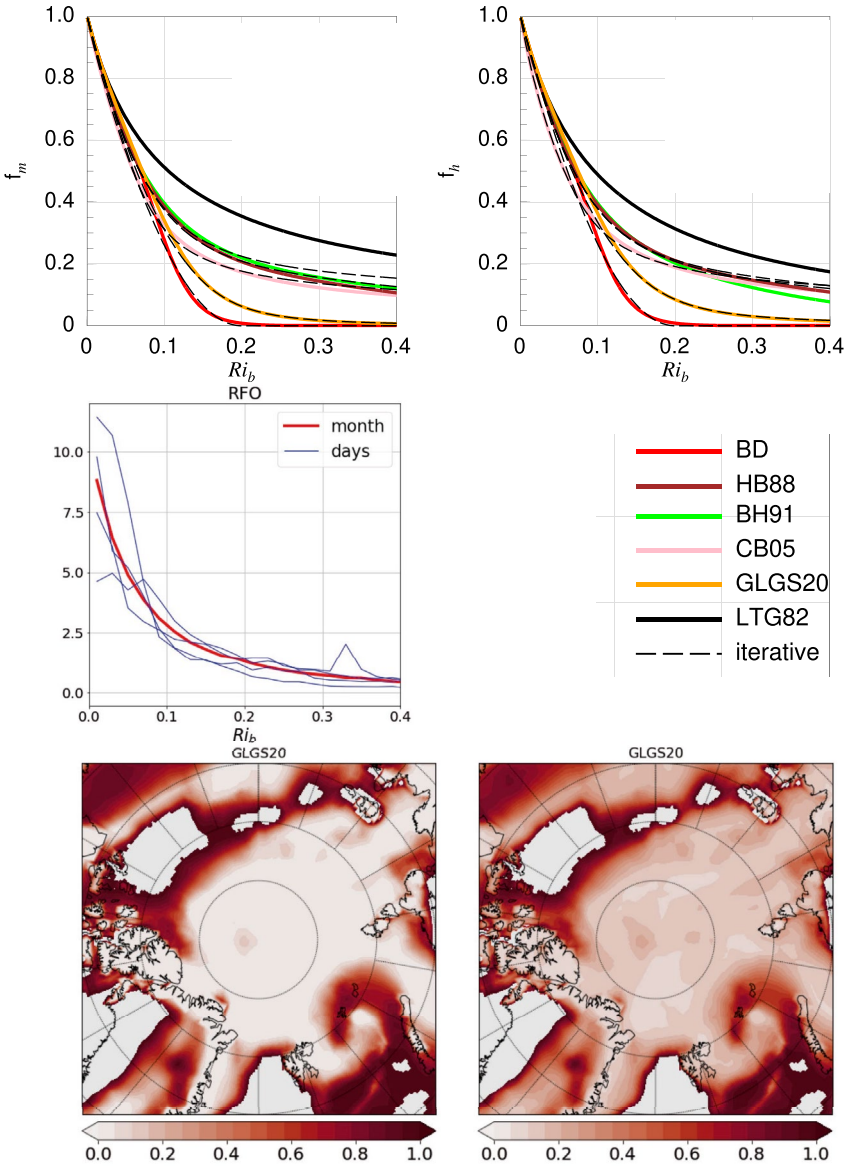

Figure 2. Top: Normalized transfer coefficients f_m and f_h for momentum and heat as a function of Ri_b. The parametrizations were obtained as a solution of the MOST Equations 4–10 using the stability correction Equations 11–16. Middle: Relative frequency of occurrence of Ri_b on March 1, 10, 20, and 30, 2019 (blue) and of entire March 2019 (red) for the region shown in the bottom panel. Values are based on ERA-Interim data archive (Berrisford et al., 2011). Bottom: Normalized transfer coefficients f_m (left) and f_h (right) at 10 m height for stable stratification based on the SCFs of GLGS20. The Arctic region is shown using ERA-Interim data for March 2019.

with $c_1 = c_2 = 10$, which is currently used, for example, in the HIRHAM5 (Christensen et al., 2007) and the ECHAM6-FESOM models (Sidorenko et al., 2015). The figure shows that overall the parametrization of LTG82 provides the largest transfer coefficients of all considered here.

For comparison of the parametrizations, we show in Figure 2 results for LTG82 and all five members of the package, taken for the same typical conditions as in Figure 1. The figure shows that the normalized transfer coefficients f_m and f_h based on the BD SFs are zero in the range $Ri_b > Ri_{b,cr}$, where $Ri_{b,cr} = 0.2$ is the critical bulk Richardson number. Thus the BD f_m and f_h functions represent cutoff functions while the other ones are short-tail or long-tail functions. If a function is decaying as $1 / Ri_b^3$ at $Ri_b \to \infty$, or faster, it is called a short-tail function, but it is called a long-tail function if the decay is slower, sf. LTG82. It is obvious

that the differences between the short-tail and long-tail transfer coefficients are largest at large Ri_b, so that their largest effect on fluxes can be expected also at large Ri_b. The simple analysis of Equations 6–10 using Table 1 shows that the tails are long for normalized transfer coefficients based on LTG82, HB88, BH91, and CB05. On the contrary, the parametrization based on GLGS20 resulted in short-tail functions. The quite similar values in Table 1 of γ and ζ_a for HB88, BH81, and CB05 show that our approach correctly captures the fact that these functions and corresponding transfer coefficients belong to the same group, namely long-tail functions. In contrast, the values of γ and ζ_a for BD and GLGS20 significantly differ from each other and from those for HB88, BH81, and CB05, indicating that the functions belong to three different groups in good agreement with the iterative solution.

Figure 2 (top) documents that for small $Ri_b < 0.07$ all normalized transfer coefficients have the same good quality in representing results of GLGS20. Vice versa, for large Ri_b, all normalized transfer coefficients show large differences to the results from GLGS20. Since SF of GLGS20 are the most accurate in representing the SHEBA measurements, one can conclude that f_m and f_h based on BD underestimate measurements, but LTG82 and HB88, BH91, and CB05 SFs overestimate measurements for large Ri_b.

5. Illustrating Example of the Stability Impact on Normalized Transfer Coefficients

To get an impression on the temporal and geographic distribution of the stability impact on the normalized transfer coefficients f_m and f_h and to hint to possible effects in NWP and climate models, we consider Era Interim data (Berrisford et al., 2011) of March 2019 and evaluate first the relative frequency of occurrence (RFO) of Ri_b for this month and several days (March 1, 10, 20, and 30). The distributions can be considered as typical for late winter/early spring conditions (see Figure 2, middle panel). Additionally, the Arctic wide geographic distributions of normalized transfer coefficients f_m and f_h are shown as well for one representative day (March 20) (see Figure 2, bottom panel). Although this is just one diagnostic example, we found that the principle effects shown here and described below are representative for the cold seasons.

The RFOs (normalized to unity for $Ri_b \geq 0$) in Figure 2 show that the near-neutral ($0 \leq Ri_b < 0.02$), weakly stable ($0.02 \leq Ri_b < 0.1$), very stable ($0.1 \leq Ri_b < 0.4$) surface layers are present in the Arctic region. The monthly RFO (red curve) shows that the probability of occurrence of both near-neutral and weakly stable layers is nearly the same as the probability of the very stable layers. The reason is that although the RFO monotonically decreases when Ri_b increases, the range of Ri_b for the very SSL is larger. The figure also shows that the dispersion of the monthly RFO is relatively large, see daily RFO (blue curves) for March 1, 10, 29, and 30. Overall, the comparison of RFOs (Figure 2, middle) with normalized transfer coefficients f_m and f_h (Figure 2, top) reveals that using transfer coefficients based on other SFs than those derived on the basis of polar measurements (i.e., SFs of GLGS20) can significantly overestimate the actual turbulent fluxes of momentum and heat. The main overestimation takes place for very SSLs (in the range $Ri_b > 0.1$).

The Arctic wide distribution of the normalized transfer coefficients f_m and f_h (Figure 2, bottom) based on the SFs of GLGS20 show that the coefficients are small in the central Arctic region (latitudes larger than 75° N), where the surface layer is very stable (large Ri_b). These small values cover a huge region, which demonstrates the importance of a realistic choice of the f_m and f_h functions not only for near-neutral but also for strongly stable conditions. In the southern areas, values are larger because of often near-neutral stratification, but also here very stable regions can occur depending on the regimes with either off-ice or on-ice flow (cold-air outbreaks or warm-air intrusions). The figure shows an example of an approaching cyclone between Svalbard and Novaja Semlja which obviously has a large impact on stability.

Figure 3 presents the difference $f_m - f_{m,GLGS}$ and $f_h - f_{h,GLGS}$ of GLGS20 to the other members of the package. It can be seen that HB88, BH91, and CB05 show largely positive differences in the Central Arctic and in the neighboring areas. The largest positive differences are found in CB05 where they reach above 0.2 for both f_m and f_h in the areas where Ri_b is larger than 0.1. The opposite behavior is found for BD, which shows negative differences for the range $0.1 < Ri_b < 1.2$ and only minor differences everywhere else. They are presented as filamentary patterns because the corresponding normalized transfer coefficients approach f_m and f_h of GLGS20 in both limits of small and large Ri_b. Negative differences in the same range of Ri_b are

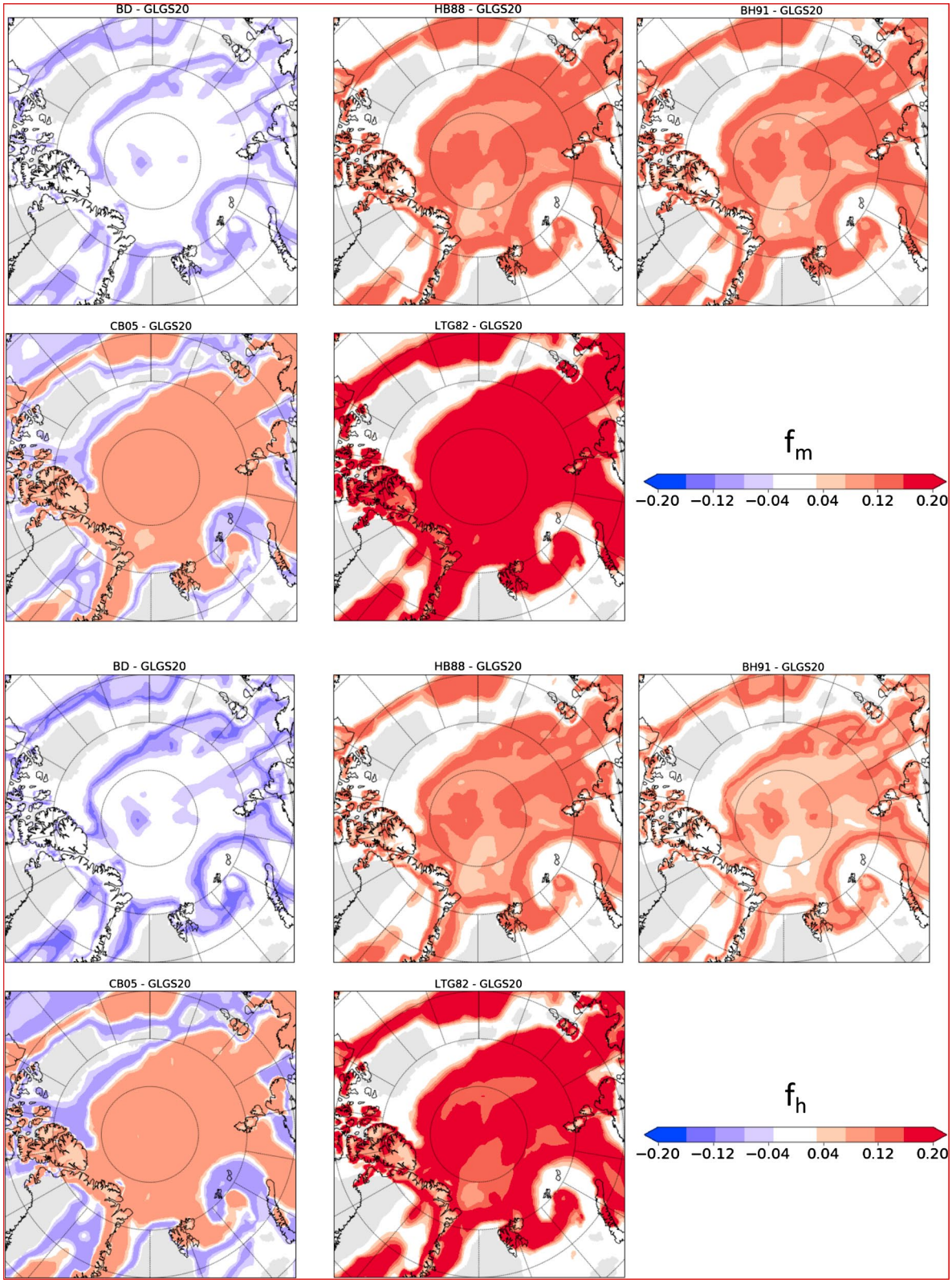

Figure 3. Differences $f_m - f_{m,GLGS}$ and $f_h - f_{h,GLGS}$ at 10 m height for March 20, 2019 where f_m and f_h are the normalized transfer coefficients referring to GLGS20 (Equations 15 and 16) and f_m and f_h refer to all other members of the package (Equations 11–14) and to the parametrization of LTG82 (Equation 17).

also found in CB05. There, however, the differences are positive in the areas where $Ri_b > 0.15$. According to Equations 4 and 5 the patterns of C_d and C_h are similar to the patterns of f_m and f_h.

6. Discussion

In this section, we discuss the advantages and shortcomings of our non-iterative parametrizations and compare the parametrizations with those suggested earlier.

6.1. Advantages and Shortcomings of Non-Iterative Parametrizations

The relevance of a non-iterative scheme and its advantages have been addressed by, for example, Grachev and Fairall (1997), Andreas et al. (2010), Li et al. (2014), and GLGS20.

The number of iterations of an iterative scheme and thus the numerical costs depend on the required precision and initial values for the iteration. In agreement with Andreas et al. (2010), Jiménez et al. (2012), and Li et al. (2014), we found that for an accuracy of 0.1% typically 5 iterations are needed by an iterative scheme for $0 \le \zeta < 2$ while 20 iterations can become necessary when ζ approaches 100. In models with very small time steps, however, and when they save values from the preceding time step, iteration is required only in the model's initialization phase and in case of strong nonstationarity (Li et al., 2014). But the iterative schemes require a large number of iterations, especially in climate models with large time steps so that the solution of the preceding time step is far away from the new solution. Then the application of a non-iterative method saves computational costs for the flux determination in the order of $(N-1)t_i$ where N is the required number of iterations and t_i the required cpu-time in one iteration. Moreover, non-iterative parametrizations are useful for a proper choice of an initial guess when they are used in combination with iterative schemes (Grachev & Fairall, 1997).

However, all non-iterative schemes also have shortcomings. Namely, while iterative solutions can represent almost an exact mathematical solution of the MOST equations with prescribed precision (e.g., 0.1%), non-iterative schemes (parametrizations) have a finite and fixed error due to approximations used for their derivation. However, this disadvantage is of minor importance keeping in mind the physical uncertainty of the SFs. The latter is always present due to the uncertainties of measurements (often $20-30\%$, see Businger et al. (1971), Dyer (1974), and GLGS20). As we have shown in Section 4, the parametrizations which we derived have higher accuracy at small Ri_b and a maximal error of $10-30\%$ depending on the SCF occurs only at large values of Ri_b and in the cases with extreme surface roughness (Figure 1). This accuracy is sufficient for an adequate representation of the impact of stratification on the unresolved turbulent mixing processes in the SSL.

6.2. Comparison With Earlier Parametrizations

The key point of any non-iterative parametrization of transfer coefficients is the parametrization of the $\zeta - Ri_b$ relationship. A large number of such parametrizations exist for both stable and unstable surface layers, but none of them has a similar universality as our proposed scheme since they were all derived for individual SCFs only (see, e.g., Blümel, 2000; Launiainen, 1995; Li et al., 2010, 2014; Sharan & Srivastava, 2014; Yang et al., 2001; Wouters et al., 2012). Below, we consider only those parametrizations, which are based on the SCFs of HB88, BH91, and CB05 which are the relevant ones for our study of SSL. These are parametrizations of Launiainen (1995), Li et al. (2010), Wouters et al. (2012), and Li et al. (2014) (La95, Li10, Wo12, and Li14, respectively). To discuss their main advantages and shortcomings, the original parametrizations are presented here in a functional form, which is convenient for an intercomparison. The new form is obtained by rearranging the terms of the original formulas and by redefining notations for the independent variables and parameters.

The parametrization of La95, which is based on the SFs of HB88, is given by

$$\zeta = \begin{cases} [\ln\epsilon_m(1-5.2\,Ri_b)^{-1} + 1.3\ln\alpha]\,Ri_b, & 0 < Ri_b \le 0.08, \\ (1.18\ln\epsilon_m + 1.5\ln\alpha - 1.37)\,Ri_b + & \\ (1.89\ln\epsilon_m + 44.2)\,Ri_b^2, & 0.08 < Ri_b \le 0.2 \end{cases}, \tag{18}$$

where $\alpha = \epsilon_t/\epsilon_m$. This parametrization is often used in models. For a review and discussion of drawbacks such as the occurrence of discontinuities at the interval limits of the different polynomials we refer to GL18. We stress, that the discontinuities are generated then also in normalized transfer coefficients, which are based on Equation 18. Thus, the parametrizations of La95 do not satisfy the criteria (1), (2), and (4).

The parametrization of Li10 for the SFs of BH91 is given by the equation

$$\zeta = \begin{cases} [(-b_{w11}\ln\alpha + b_{w12})\ln\epsilon_m + (-b_{w21}\ln\alpha + b_{w22})]\,Ri_b + & \\ [(-a_{w11}\ln\alpha + a_{w12})\ln\epsilon_m + (-a_{w21}\ln\alpha + a_{w22})]\,Ri_b^2, & 0 < Ri_b \le 0.2, \\ b_{s11}\ln\epsilon_m - b_{s21}\ln\alpha + b_{s22} + (a_{s11}\ln\epsilon_m + a_{s21})Ri_b, & Ri_b > 0.2. \end{cases} \tag{19}$$

Here, the subscript "w" refers to the region with weak stratification $0 < Ri_b \le 0.2$ and "s" to the region with strong stratification $Ri_b > 0.2$ and $\alpha = \epsilon_m / \epsilon_t$ as before. Numerical values of the 13 coefficients are: $a_{w11} = 0.5738$, $a_{w12} = -0.4399$, $a_{w21} = -4.901$, $a_{w22} = 52.50$, $b_{w11} = -0.0539$, $b_{w12} = 1.540$, $b_{w21} = -0.6690$, and $b_{w22} = -3.282$. Other coefficients are: $a_{s11} = 0.7529$, $a_{s21} = 14.94$, $b_{s11} = 0.1569$, $b_{s21} = -0.3091$, and $b_{s22} = -1.303$.

The main disadvantages of the Li10 parametrization are the same as that of La95. Both parametrizations do not satisfy the criteria (1), (2), and (4). The Li10 parametrization has a discontinuity at $Ri_b = 0.2$, which is clearly visible in Figure 4 of GL18. The Li10 and La95 parametrizations are well suited for lookup table algorithms, but are not appropriate for algorithms relying on continuous analytical functions.

The parametrizations of Wo12 and Li14 for SFs of CB05 are given below. Strictly, Wo12 and Li14 considered generalized MOST functions, which were corrected at small ζ by terms describing the effect of the roughness sublayer. These corrections are significant for very rough surfaces (urban boundary layer), but not for polar sea ice conditions. Here, we present their result only for the limiting case of negligible corrections due to the roughness sublayer. The parametrization suggested by Wo12 has the functional form:

$$\zeta = \begin{cases} Eq.(21), & 0 < \zeta \le \zeta_t, \\ \zeta_t + D(\zeta_t)\left(Ri_b - Ri_{b,t}\right), & \zeta \ge \zeta_t \end{cases} \tag{20}$$

where

$$\zeta = \frac{\left[(\ln\epsilon_t - 2a_m\ln\epsilon_m Ri_b)^2 + 4\ln^2\epsilon_m(a_h - a_m^2 Ri_b)Ri_b\right]^{1/2} - (\ln\epsilon_t - 2a_m\ln\epsilon_m Ri_b)}{2(a_h - a_m^2 Ri_b)}, \tag{21}$$

the value $\zeta = \zeta_t$, separating the regions of weak $0 < \zeta \le \zeta_t$ and strong $\zeta \ge \zeta_t$ stratification, is given as

$$\zeta_t = -0.316 - \frac{0.515}{\epsilon_t} + \frac{25.8}{\epsilon_t^2} + \frac{4.36}{\ln\epsilon_t} - \frac{6.39}{\ln^2\epsilon_t} + \frac{0.834}{\ln\ln\epsilon_m} - \frac{0.0267}{\ln^2\ln\epsilon_m}. \tag{22}$$

The slope function $D(\zeta_t)$ is given by the equation

$$D(\zeta_t) = \frac{\left[\ln\epsilon_m + a_m(1-1/\epsilon_m)\zeta_t\right]^3}{\ln\epsilon_m\ln\epsilon_t + \left[2a_h(1-1/\epsilon_t)\ln\epsilon_t - a_m(1-1/\epsilon_m)\ln\epsilon_m\right]\zeta_t} \tag{23}$$

Table 2
Comparison With Earlier Parametrizations

	1	2	3	4	5	6	Equations
La95 (HB88)	−	−	+	−	+	+	4–7, 12, 18
Li10 (BH91)	−	−	+	−	+	+	4–7, 12, 13, 19
Wo12 (CB05)	+	−	+	+	+	−	4–7, 14, 20–24
Li14 (CB05)	+	−	+	+	+	−	4–7, 14, 25
GLSG21 (BD, HB88, BH91, CB05, GLGS20)	+	+	+	+	+	+	4–9, 11–16

Note. La95, Li10, Wo12, Li14, and GLSG21 refer to the parametrizations of Launiainen (1995), Li et al. (2010), Wouters et al. (2012), Li et al. (2014), and this study, respectively. BD, HB88, BH91, CB05, and GLGS20 refer to the stability correction functions of Businger et al. (1971), Dyer (1974), Holtslag and De Bruin (1988), Beljaars and Holtslag (1991), Cheng and Brutsaert (2005), and Gryanik et al. (2020), respectively. Columns are the quality criteria 1–6 which are formulated in Section 2 for all parametrizations.

with

$$a_m = 4.76 + \frac{7.03}{\epsilon_m} + \frac{0.24\epsilon_m}{\epsilon_t}, \quad a_h = 5. \tag{24}$$

The same a_m and a_h are also used in Equation 21 describing the region of weak stability.

The Equation 20 is a continuous function at $\zeta = \zeta_t$ and has a continuous derivative. However, the parametrizations of Wo12 do not satisfy the criteria (2) and (6).

The parametrization of Li14 has the functional form

$$\zeta = Ri_b \sum_{i=0}^{1} \sum_{j,k=0}^{3} c_{ijk} Ri_b^i \ln \epsilon_m^j (\ln \epsilon_t - \ln \epsilon_m)^k \tag{25}$$

where the summation is performed under the constraint $i + j + k \leq 4$. The function Equation 25 is obtained by applying a universally applicable regression method, which is based on splitting the range $0 < Ri_b < 0.25$ into 13 intervals. Thus the parametrization represents a piece-vice function given by second order polynomials in Ri_b for each of the 13 intervals. The coefficients c_{ijk} are provided as a table (see Li14 for all details). Li14 showed that their parametrization has high accuracy and is more accurate than that of Wo12. We show in Appendix A that our approach can be reformulated so that it is formally similar to Equation 25. However, note that Equation 25 is valid so far only for one set of SCFs, wile our approach is universal (see above).

Summarizing (see Table 2), we conclude that in contrast to the parametrizations of La95 and Li10, but in agreement with Wo12 and Li14, the parametrizations (4)–(10) represent a continuous function in Ri_b for all values of ϵ_m and ϵ_t. None of the parametrizations with the exception of GL18 and GLGS20 satisfy all the criteria (1)–(6). Moreover, except the approaches by Li14, GL18, and GLGS20, none of the other approaches is derived in a universal mathematical framework. The formal mathematical relation of the approach based on Equations 4–10 to the approach of Li14 is discussed in Appendix A.

7. Concluding Remarks

The most important results can be summarized as follows:

1. Non-iterative parametrizations of momentum and heat transfer coefficients for the SSL were derived for five pairs of SFs, which are summarized in Table 1. Altogether the parametrizations cover the entire range of Ri_b,ϵ_m and ϵ_t as observed during the most famous and most comprehensive campaigns for atmospheric surface layer conditions over sea-ice and land. The parametrizations have a simple analytical functional form.
2. The new non-iterative surface flux parametrizations are presented in a package, which is well suited for practical use in models, especially for those relying already now on aggregated schemes of transfer coefficients (e.g., two or three members of the package). Despite the different functional forms of the

SFs, the related transfer coefficients are given for the first time in a universal framework for all members of the package.

We stress that the difference of transfer coefficients between members of the package is small only at small Ri_b, but is large at large Ri_b. Correspondingly, the differences of related turbulent fluxes of momentum and heat are large too.

The basis for the derivation of the new non-iterative parametrizations had been presented by Gryanik and Lüpkes (2018). We have shown now that this method of derivation is flexible. Thus, new SFs can be added to the package and only two parameters γ and ζ_a have to be adjusted for each pair of SFs.

An important step toward a generalization of the non-iterative parametrizations could be accounting for the flux-dependence of roughness lengths, which is important for the calculation of turbulent fluxes over the ocean and in the roughness sublayer over complex terrains. Moreover, a combination with parametrizations allowing variable roughness as, for example, the scheme by Lüpkes and Gryanik (2015) for future research.

Finally, we hope that the new non-iterative parametrizations can be used in future studies as a basis for a simple and economic, systematic quantification of the impact of surface layer turbulent fluxes on the uncertainty of results in NWP and climate models, and also, for intercomparison studies.

Appendix A: Representation of the New Parametrizations by a Taylor Series Expansion

The parametrization (9) in the main text, can be rewritten in a functional form, which is very close to that used by Li14, see Equation 25. To this end one can expand the coefficient $A(\epsilon_m, \epsilon_t)$ in form of a Taylor series in the parameters $\mu = \ln\epsilon_m/(-\psi_{ma}) > 0$ and $\mu_t = \ln\epsilon_t/(-\psi_{ha}) > 0$ (note that $-\psi_{ma} > 0$ and $-\psi_{ha} > 0$ for stable conditions) using the well known formula

$$\left(1+x\right)^a = \sum_{j=0}^{\infty} \frac{(a-j)!}{j!} x^j, \tag{A1}$$

where $(a-j)! = a(a-1)\ldots(a-j)$ and $0! = 1$ by definition. The result is

$$A = \zeta_a \sum_{j,k=0}^{\infty} c_{jk}^{(\gamma)} \ln\epsilon_m^j \ln\epsilon_t^k - \frac{\ln^2\epsilon_m}{\ln\epsilon_t} \sum_{j,k=0}^{\infty} c_{jk}^{(\gamma-1)} \ln\epsilon_m^j \ln\epsilon_t^k, \tag{A2}$$

where

$$c_{jk}^{(\gamma)} = \zeta_a^{\gamma} \frac{(-\psi_{ma})^{2\gamma-j}}{(-\psi_{ha})^{\gamma+k}} \frac{(2\gamma-j)!(-\gamma-k)!}{j!k!} \tag{A3}$$

After substituting Equations A2 with A3 in Equation 9 and rearranging the terms one finds the stability parameter as

$$\zeta = Ri_b \left[\frac{\ln^2\epsilon_m}{\ln\epsilon_t} + Ri_b^{\gamma-1} \left(\sum_{j,k=0}^{\infty} \zeta_a c_{jk}^{(\gamma)} \ln^j\epsilon_m \ln^k\epsilon_t - \sum_{j,k=0}^{\infty} c_{jk}^{(\gamma-1)} \ln^{j+2}\epsilon_m \ln^{k-1}\epsilon_t \right) \right] \tag{A4}$$

The reformulation of our parametrizations in the functional form (A4) shows similarities and differences to Equation 25 of Li14. In general, the convergence of the series (A2) can be very slow, when the parameters of the expansion μ and μ_t are not small enough. However, a further improvement can be achieved by an approach similar to Li14, which is based on splitting the Ri_b range into a large number of intervals (order of 10) and using Equation A2 in each interval separately. We leave this idea for a future study.

Data Availability Statement

The data used for this study are accessible under https://www.ecmwf.int/en/elibrary/8174-era-interim-archive-version-20.

Acknowledgments
The authors are glad to thank Drs. W. Dorn, N. Koldunov, and S. Losa for suggestions and comments. The authors gratefully acknowledge the funding by the Helmholtz Association (Germany) and the Russian Science Foundation in the priority thematic area of Climate Research (Project HRSF-0036), and the support by Helmholtz Climate Initiative REKLIM (Regional Climate Change). Part of the study was also funded by the Deutsche Forschungsgemeinschaft (DFG; German Research Foundation) Project 268020496 TRR 172, within the Transregional Collaborative Research Center Arctic Amplification ($(AC)^3$). Open access funding enabled and organized by Projekt DEAL.

References

Andreas, E. L. (2002). Parameterizing scalar transfer over snow and ice: A review. *Journal of Hydrometeorology*, *3*(4), 417–432. https://doi.org/10.1175/1525-7541(2002)003<0417:pstosa>2.0.co;2

Andreas, E. L., Horst, T. W., Grachev, A. A., Persson, P. O. G., Fairall, C. W., Guest, P. S., & Jordan, R. E. (2010). Parametrizing turbulent exchange over summer sea ice and the marginal ice zone. *Quarterly Journal of the Royal Meteorological Society*, *136*(649), 927–943. https://doi.org/10.1002/qj.618

Beljaars, A., & Holtslag, A. A. M. (1991). Flux parameterization over land surfaces for atmospheric models. *Journal of Applied Meteorology and Climatology*, *30*(3), 327–341. https://doi.org/10.1175/1520-0450(1991)030<0327:fpolsf>2.0.co;2

Berrisford, P., Dee, D., Poli, P., Brugge, R., Fielding, K., Fuentes, M., et al. (2011). *The ERA-Interim archive, version 2.0 (ERA report series. 1. Technical Report, p. 23). ECMWF.*

Blümel, K. (2000). An approximate analytical solution of flux-profile relationships for the atmospheric surface layer with different momentum and heat roughness lengths. *Boundary-Layer Meteorology*, *97*(2), 251–271. https://doi.org/10.1023/a:1002708313017

Bou-Zeid, E., Anderson, W., Katul, G. G., & Mahrt, L. (2020). The persistent challenge of surface heterogeneity in boundary-layer meteorology: A review. *Boundary-Layer Meteorology*, *177*(2), 227–245. https://doi.org/10.1007/s10546-020-00551-8

Businger, J. A., Wyngaard, J. C., Izumi, Y., & Bradley, E. F. (1971). Flux-profile relationships in the atmospheric surface layer. *Journal of the Atmospheric Sciences*, *28*(2), 181–189. https://doi.org/10.1175/1520-0469(1971)028<0181:fprita>2.0.co;2

Cheng, Y., & Brutsaert, W. (2005). Flux-profile relationships for wind speed and temperature in the stable atmospheric boundary layer. *Boundary-Layer Meteorology*, *114*(3), 519–538. https://doi.org/10.1007/s10546-004-1425-4

Christensen, O. B., Drews, M., Christensen, J. H., Dethloff, K., Ketelsen, K., Hebestadt, I., & Rinke, A. (2007). *The HIRHAM regional climate model. Version 5 (beta).* Danish Climate Centre, Danish Meteorological Institute.

Deardorff, J. W. (1968). Dependence of air-sea transfer coefficients on bulk stability. *Journal of Geophysical Research: Atmospheres*, *73*(8), 2549–2557. https://doi.org/10.1029/jb073i008p02549

Dyer, A. (1974). A review of flux-profile relationships. *Boundary-Layer Meteorology*, *7*(3), 363–372. https://doi.org/10.1007/bf00240838

Elvidge, A. D., Renfrew, I. A., Weiss, A. I., Brooks, I. M., Lachlan-Cope, T. A., & King, J. C. (2016). Observations of surface momentum exchange over the marginal ice zone and recommendations for its parametrisation. *Atmospheric Chemistry and Physics*, *16*(3), 1545–1563. https://doi.org/10.5194/acp-16-1545-2016

Grachev, A. A., Andreas, E. L., Fairall, C. W., Guest, P. S., & Persson, P. O. G. (2007). SHEBA flux-profile relationships in the stable atmospheric boundary layer. *Boundary-Layer Meteorology*, *124*(3), 315–333. https://doi.org/10.1007/s10546-007-9177-6

Grachev, A. A., & Fairall, C. W. (1997). Dependence of the Monin-Obukhov stability parameter on the bulk Richardson number over the ocean. *Journal of Applied Meteorology and Climatology*, *36*(4), 406–414. https://doi.org/10.1175/1520-0450(1997)036<0406:dotmos>2.0.co;2

Gryanik, V. M., & Lüpkes, C. (2018). An efficient non-iterative bulk parametrization of surface fluxes for stable atmospheric conditions over polar sea-ice. *Boundary-Layer Meteorology*, *166*(2), 301–325. https://doi.org/10.1007/s10546-017-0302-x

Gryanik, V. M., Lüpkes, C., Grachev, A., & Sidorenko, D. (2020). New modified and extended stability functions for the stable boundary layer based on SHEBA and parametrizations of bulk transfer coefficients for climate models. *Journal of the Atmospheric Sciences*, *77*, 2687–2716. https://doi.org/10.1175/jas-d-19-0255.1

Holtslag, A. A. M., & De Bruin, H. A. R. (1988). Applied modeling of the nighttime surface energy balance over land. *Journal of Applied Meteorology and Climatology*, *27*(6), 689–704. https://doi.org/10.1175/1520-0450(1988)027<0689:amotns>2.0.co;2

Jiménez, P. A., Dudhia, J., González-Rouco, J. F., Navarro, J., Montávez, J. P., & García-Bustamante, E. (2012). A revised scheme for the WRF surface layer formulation. *Monthly Weather Review*, *140*(3), 898–918. https://doi.org/10.1175/mwr-d-11-00056.1

Jung, T., Gordon, N. D., Bauer, P., Bromwich, D. H., Chevallier, M., Day, J. J., et al. (2016). Advancing polar prediction capabilities on daily to seasonal time scales. *Bulletin of the American Meteorological Society*, *97*(9), 1631–1647. https://doi.org/10.1175/bams-d-14-00246.1

Lüpkes, C., & Gryanik, V. M. (2015). A stability-dependent parametrization of transfer coefficients for momentum and heat over polar sea ice to be used in climate models. *Journal of Geophysical Research: Atmospheres*, *120*(2), 552–581. https://doi.org/10.1002/2014jd022418

Launiainen, J. (1995). Derivation of the relationship between the Obukhov stability parameter and the bulk Richardson number for flux-profile studies. *Boundary-Layer Meteorology*, *76*(1), 165–179. https://doi.org/10.1007/bf00710895

Li, Y., Gao, Z., Lenschow, D. H., & Chen, F. (2010). An improved approach for parameterizing surface-layer turbulent transfer coefficients in numerical models. *Boundary-Layer Meteorology*, *137*(1), 153–165. https://doi.org/10.1007/s10546-010-9523-y

Li, Y., Gao, Z., Li, D., Wang, L., & Wang, H. (2014). An improved non-iterative surface layer flux scheme for atmospheric stable stratification conditions. *Geoscientific Model Development*, *7*(2), 515–529. https://doi.org/10.5194/gmd-7-515-2014

Louis, J., Tietke, M., & Geleyn, J. (1982). A short history of the operational PBL-parameterization at ECMWF. *Paper presented at the ECMWF Workshop on Planetary Boundary Layer Parameterization* (pp. 59–79).

Monin, A., & Obukhov, A. (1954). Basic laws of the turbulent transport in the atmosphere surface layer. *Trudy GGI*, *24*(151), 163–186.

Schneider, T. (2020). *Impact of a changed turbulence parameterization for polar conditions in an arctic regional climate model (Unpublished master's thesis)* (p. 92). University Potsdam. Retrieved from https://drive.google.com/file/d/1jBp7Ek4EofSvt1iTzSkX7O6v6XGV7KHQ/view?usp=sharing

Sharan, M., & Kumar, P. (2011). Estimation of upper bounds for the applicability of non-linear similarity functions for non-dimensional wind and temperature profiles in the surface layer in very stable conditions. *Proceedings of the Royal Society A: Mathematical, Physical & Engineering Sciences*, *467*(2126), 473–494. https://doi.org/10.1098/rspa.2010.0220

Sharan, M., & Srivastava, P. (2014). A semi-analytical approach for parametrization of the Obukhov stability parameter in the unstable atmospheric surface layer. *Boundary-Layer Meteorology*, *153*(2), 339–353. https://doi.org/10.1007/s10546-014-9948-9

Sidorenko, D., Rackow, T., Jung, T., Semmler, T., Barbi, D., Danilov, S., et al. (2015). Towards multi-resolution global climate modeling with ECHAM6–FESOM. Part I: Model formulation and mean climate. *Climate Dynamics*, *44*(3–4), 757–780. https://doi.org/10.1007/s00382-014-2290-6

Srivastava, P., & Sharan, M. (2019). Analysis of dual nature of heat flux predicted by Monin-Obukhov similarity theory: An impact of empirical forms of stability correction functions. *Journal of Geophysical Research: Atmospheres*, *124*(7), 3627–3646. https://doi.org/10.1029/2018jd029740

Wouters, H., De Ridder, K., & van Lipzig, N. P. (2012). Comprehensive parametrization of surface-layer transfer coefficients for use in atmospheric numerical models. *Boundary-Layer Meteorology*, *145*(3), 539–550. https://doi.org/10.1007/s10546-012-9744-3

Yang, K., Tamai, N., & Koike, T. (2001). Analytical solution of surface layer similarity equations. *Journal of Applied Meteorology and Climatology*, *40*(9), 1647–1653. https://doi.org/10.1175/1520-0450(2001)040<1647:asosls>2.0.co;2